Title
Efficacy of Intraperitoneal Administration of PEGylated NELL-1 for Bone Formation

Author
Tanjaya, Justine

Publication Date
2015

Peer reviewed|Thesis/dissertation

UNIVERSITY OF CALIFORNIA

Los Angeles

Efficacy of Intraperitoneal Administration of PEGylated NELL-1 for Bone Formation

A thesis submitted in partial satisfaction

Of the requirements for the degree

Master of Science in Oral Biology

By

Justine Tanjaya

2015

ABSTRACT OF THESIS

Efficacy of Intraperitoneal Administration of PEGylated NELL-1 for Bone Formation

By

Justine Tanjaya

Master of Science in Oral Biology

University of California, Los Angeles, 2015

Professor Kang Ting, Chair

Background: Systemically delivered NELL-1, a potent pro-osteogenic protein, promotes bone formation in healthy and osteoporotic mouse models. PEGylation of NELL-1 (NELL-PEG) increases the half-life of the protein in a mouse model without compromising its osteogenic potential, thereby improving its pharmacokinetics upon systemic delivery. Weekly intravenous (IV) NELL-PEG injection significantly enhances overall bone properties. This study consists of a two-fold approach; a biodistribution test and an *in vivo* osteogenic potential test. The biodistribution test compared two commonly used administration methods

for drug delivery other than IV – intraperitoneal (IP) and subcutaneous (SC) – to examine NELL-PEG biodistribution in mice.

Methods: To investigate the biodistribution of NELL-PEG protein for various administration methods, nine female CD-1 adult mice were randomly divided into 3 groups (one group of NELL-PEG injection via IP administration, one group of NELL-PEG injection via SC injection, and one PBS control group). Animals were subjected to either 100 µl of NELL-PEG solution via IP injection (1.25 mg/kg), NELL-PEG solution via SC injection (1.25 mg/kg) injection or assigned to the control group with PBS solution injection. The second part of the biodistribution study was performed to compare the protein distribution of NELL-PEG injection via IP administration at two different time points (48h and 72h) post-injection. Nine female CD-1 adult mice were randomly divided into 3 groups (two groups of NELL-PEG injection via IP administration and one PBS control group). Animals were either administered with 100 µl of NELL-PEG solution via IP injection (2x dose of 2.5 mg/kg) or assigned to the control group with PBS solution injection. The first group of NELL-PEG-treated animals was sacrificed at 48h post-injection, while the second group was sacrificed at 72h.

For the *in vivo* study, fourteen female C57BL/6J adult mice were randomly distributed into NELL-PEG group and PBS control group, and were injected with either NELL-PEG (2.5mg/kg) or PBS intraperitoneally. Subsequently, changes in bone mineral density were monitored every two weeks with Dual energy X-ray absorptiometry (DEXA). Simultaneously, all animals were injected with 18F-NaF ion probe and underwent microPET scan to monitor the dynamic changes of

bone turnover rate. At the end of the treatment, all animals were sacrificed and bone tissues such as femurs, tibias, and vertebrae were scanned with micro-Computed Tomography (microCT). Finally, immunohistochemistry was performed to confirm the anabolic and anti-resorptive effect of NELL-PEG injection via the IP route on the bone remodeling process.

Results: Compared to a single-dose SC injection (1.25 mg/kg), a single-dose IP administration yielded a higher protein uptake in the targeted bone sites. When the IP injection dose was doubled to 2.5 mg/kg, the protein remained in the femurs, tibias, and vertebrae for up to 72 hours. Next, based on the results of the biodistribution study, IP administration was selected to further investigate the *in vivo* osteogenic effects of weekly NELL-PEG injection (q7d). *In vivo*, the IP administered NELL-PEG group showed significantly greater bone mineral density (BMD), bone volume fraction (BV/TV), and trabecular bone formation in the targeted bone sites compared to the PBS control. Based on the histological findings, we also observed that upon NELL-PEG IP administration, there is a significantly higher osteoblasts activity with lower osteoclasts activity.

Conclusion: In summary, our results indicate that NELL-PEG injection via the IP administration route revealed a higher uptake when compared to the SC group, with high protein retention at the multiple skeletal sites such as calvaria, vertebral body, and femur. Additionally, weekly intraperitoneal administration of double dose NELL-PEG successfully improves overall bone quality by increasing BMD, inducing a high activity of bone remodeling process, and promoting robust bone formation while reducing bone resorption, which is similar to the single dose of

NELL-PEG injection via the IV route results. Altogether, these findings provide a strong rationale for selecting IP administration route as a preferable method for NELL-PEG systemic injection for osteoporosis therapy.

The thesis of Justine Tanjaya is approved.

Reuben Kim

Shen Hu

Xinli Zhang

Kang Ting, Committee Chair

University of California, Los Angeles

2015

This thesis is dedicated to

All of the mentors for their academic guidance

the entire lab mates who have contributed to this project

and my family and friends

who have supported me throughout my life.

TABLE OF CONTENTS

LIST OF FIGURES

Acknowledgements

This study was supported by the Center for the Advancement of Science in Space and the National Aeronautics and Space Administration (CASIS-NASA) 09-253-0369, NIH/NIAMS R01 AR061399-01A1, and NIH/NIAMS R01 AR066782-01. The authors would also like to thank Dr. David Stout, PhD and Dr. Jason Lee, PhD from the UCLA California NanoSystems Institute, Andy Lin from the Statistical Consulting Group at the UCLA Institute for Digital Research and Education for their insights, as well as Dr. Kevin Lee, Dr. Mahsa Dousti, Greg Asatrian, and Swati Shresta for their great contributions and continuous support.

Drs X.Z, B.W, K.T, and C.S are inventors of Nell-1 related patents. Drs. X.Z, B.W, K.T, and C.S are founders and/or board member of Bone Biologics Inc. that sublicenses Nell-1 patents from the UC Regents, who also hold equity in the company.

Efficacy of Intraperitoneal Administration of PEGylated NELL-1 for Bone Formation

INTRODUCTION

Human NEL-like molecule-1 (NELL-1), a potent growth factor that is highly specific to the osteochondral lineage, was first identified by its overexpression in the context of human unilateral craniosynostosis (UCS), a congenital cranial defect characterized by premature fusion of one of the sutures in the developing cranium [1, 2]. Over the past two decades, NELL-1 was closely studied for its local bone formation effects [3-9]; more recently, NELL-1 has demonstrated its osteogenic potential as a systemic therapy [10-12]. Mechanistically, NELL-1 affects multiple signaling pathways and has the potential to differentiate the multipotent bone mesenchymal stem cells (BMSCs) into osteoblasts by acting specifically through the Runx2 and canonical Wnt signaling pathway and activating the ERK/JNK/MAPK pathway [2, 10, 12, 13]. Simultaneously, NELL-1 suppresses adipogenesis through the peroxisome proliferator-activated receptor gamma (PPARγ) and CCAAT/enhancer-binding protein alpha (C/EBPα) pathways [14].

A recent genome-wide association study identified *NELL-1* polymorphisms in patients with reduced bone mineral density (BMD), suggesting that *NELL-1* gene polymorphisms are associated with osteoporosis [15]. Osteoporosis is a

prevalent metabolic disease that affects over 200 million people worldwide [16-18]. With an increasingly growing elderly population, who are at the greatest risk of osteoporosis and osteoporotic fractures, osteoporosis has become one of the major public health concerns [15-20]. Skeletal deterioration resulting from osteoporosis is caused by an imbalance in bone remodeling process; which is mediated by increased osteoclastic activity and decreased osteoblastic activity. Understanding the roles of intercellular regulators in the bone remodeling process is important in planning an approach to treat osteoporosis [17-21].

Existing osteoporosis therapeutic agents fall into two classes: (i) antiresorptives, such as calcitonin, estrogen, selective estrogen receptor modulators (SERM), and bisphosphonates, which slow down bone resorption, and (ii) anabolic agents, such as teriparatide parathyroid hormone (PTH 1-34 and PTH 1-84), the only Food and Drug Administration (FDA)-approved anabolic treatment agent for osteoporosis, which targets the stimulation of osteoblastic-mediated bone formation [22-26]. Among antiresorptive therapies, bisphosphonates represent the first line of treatment for osteoporosis [27]; however, common side effects such as esophageal irritation, gastrointestinal discomfort, and even transient flu-like symptoms lead to up to 20% of those who are taking the drug to discontinue it [28, 29]. In addition, bisphosphonates are associated with risk of osteonecrosis of the jaw (ONJ) [30, 31]. New therapeutics such as cathepsin K inhibitor and denosumab (anti-osteoclastic) [28], and anti-Wnt inhibitors (anti-DKK-1 and anti-sclerostin antibodies) [32, 33] have been demonstrated to

be effective for the treatment of osteoporosis. However, odanacatib, one of the few cathepsin K inhibitors that showed adequate efficiency and safety [34], was recently reported in various clinical trials to increase fracture risk [27, 35, 36]; Denosumab can induce hypocalcaemia in patients with severe renal impairment [28]; and prolonged anti-sclerostin treatment has prompted concerns about cardiovascular health and safety [27, 37]. Therefore, there is a pressing need to develop new therapies for the treatment of osteoporosis that are not only anabolic and anti-osteoclastic, but also have fewer safety concerns.

NELL-1 has demonstrated the ability to increase BMSC numbers, promote osteogenesis, and suppress osteoclastic activity and adipogenesis, with fewer adverse effects compared to existing therapies [2, 10, 38-43]. Moreover, toxicity reports of non-conjugated NELL-1 systemic administration with various doses (1.25 mg/kg/day, 2.5 mg/kg/day, and 6.25 mg/kg/day) for five consecutive days via intravenous (IV) tail injection showed no mortality, no gross pathology, and no abnormal findings in a hematology test (data not shown). Previous studies of NELL-1 suggest that local delivery of recombinant NELL-1 (rNELL-1) can act as a combined anabolic and anti-osteoclastic agent, thus reversing osteoporotic bone loss in both small and large animal models [5, 10]. When an ovariectomized (OVX) rat model was used to mimic the human osteoporotic bone loss, local delivery of NELL-1 into the femoral intramedullary cavities enhanced the bone quality and successfully prevented osteoporotic-induced bone loss [5]. Similarly, systemic delivery of rNELL-1 via IV administration demonstrated significant bone

augmentation in osteoporotic-induced mice [10]. Since osteoporosis is a systemic skeletal disorder, it is crucial for therapeutic agents to be administered systemically in order to enhance overall bone quality. Notwithstanding the proven efficacy of NELL-1 to prevent bone loss, the clinical use of systemic rNELL-1 therapy was deemed to be quite limited due to the burden of an every other day (q2d) administration schedule [10].

PEGylation is an FDA-approved method of modifying biological molecules of a protein by using covalent conjugation of polyethylene glycol (PEG) molecules [44]. It is commonly used to prolong the half-life of a protein and increase its efficacy due to the chemical properties of PEG that are non-toxic, non-immunogenic, hydrophilic, and highly flexible that make it clinically advantageous in improving the pharmacokinetic behavior of a drug [44-46]. Recently, our group has established that PEGylated NELL-1 (NELL-PEG) demonstrates higher thermal stability and prolongs systemic circulation by preserving the osteogenic effects of NELL- without any considerable cytotoxicity [11]. The applicability and safety of NELL-PEG was further examined in an *in vivo* study where its weekly systemic administration through IV tail injection resulted in increased bone mineral density (BMD), greater bone trabecular formation, and reduced bone resorption in the targeted bone sites [12].

The aforementioned studies of NELL-PEG via the IV route have successfully demonstrated the anabolic and antiresorptive functions of the protein by

promoting bone formation and reversing bone loss without undue adverse effect of immunocytotoxicity [11, 12]. However, there is no report on NELL-PEG injection via IP and SC routes. Given the benefits of greater volume administration and reduced irritation to the veins, IP and SC injections that are frequently reported to be as effective as IV injection, might be preferable to IV injection [47-51]. Furthermore, IP administration may facilitate the absorption of the protein due to the large surface area of the abdominal cavity and the abundant blood supply at the injection site, therefore serving as a slow-release and long-acting deposit of the drug. To test our hypothesis that the systemic administration of NELL-PEG via the IP route serves as a potent osteogenic therapy for preventing and treating osteoporosis, in the present study, we first compared the protein distribution of the IP and SC NELL-PEG administration methods. Next, we examined the efficacy of weekly IP NELL-PEG administration in promoting bone formation and reversing bone loss. Furthermore, an *in vivo* mouse model was used to investigate the osteogenic potential of weekly NELL-PEG injection via the IP route.

MATERIALS AND METHODS

2.1 Animals

Three-month-old female CD-1 and C57BL/6J mice were obtained from Charles River Laboratories, and maintained under standard conditions under the supervision of the Division of Laboratory Animal Medicine (DLAM) at UCLA. Animals were housed individually per cage and maintained on a 12/12-h light-dark cycle with *ad libitum* access to laboratory rodent chow and water. The animal protocol was approved by the Office of Animal Research Oversight (OARO) and the chancellor's Animal Research Committee (ARC) at UCLA.

2.2 Biodistribution Study

To investigate the biodistribution of NELL-PEG protein for various administration methods, nine female CD-1 adult mice were randomly divided into 3 groups (one group of NELL-PEG injection via IP administration, one group of NELL-PEG injection via SC injection, and one PBS control group). Animals were subjected to either 100 µl of NELL-PEG solution via IP injection (1.25 mg/kg), NELL-PEG solution via SC injection (1.25 mg/kg) injection or assigned to the control group with PBS solution injection. The second part of the biodistribution study was performed to compare the protein distribution of NELL-PEG injection via IP administration at two different time points (48h and 72h) post-injection. Nine

female CD-1 adult mice were randomly divided into 3 groups (two groups of NELL-PEG injection via IP administration and one PBS control group). Animals were either administered with 100 µl of NELL-PEG solution via IP injection (2x dose of 2.5 mg/kg) or assigned to the control group with PBS solution injection. The first group of NELL-PEG-treated animals was sacrificed at 48h post-injection, while the second group was sacrificed at 72h. The dose was calculated based on the protein content. NELL-PEG was labeled with VivoTag 680XL (PerkinElmer, MA, USA). At 48h and 72h post-injection, all mice were euthanized and the organs (liver, kidney, spleen, heart, lungs, brain, muscle, fat, ovary, calvaria, vertebrae, femur, and tibia) were harvested, weighed, and imaged with the IVIS Lumina II optical imaging system (Caliper Life Science, MA, USA). Quantification of the total amount of protein uptake by one gram of tissue weight the organs was calculated and plotted.

2.3 In vivo assessment of bone mineral density by DXA

Fourteen female C57BL/6J adult mice were randomly distributed into NELL-PEG group and PBS control group, and were injected with either NELL-PEG (2.5mg/kg) or PBS intraperitoneally. Subsequently, changes in BMD were monitored every two weeks with dual energy X-ray absorptiometry (DXA) (PIXImus2 GE Lunar Corp., Madison, WI, USA). Longitudinal assessment of the whole body (excluding head), distal femur, and lumbar vertebrae BMD (g/cm^2)

was performed every two weeks starting at the baseline until the end of the study.

2.4 In vivo assessment of bone turnover rate by live micro positron emission tomography (micro-PET/CT) scanning with ^{18}F-NaF ion

Prior to injection, all animals were warmed on a heating pad for 15 minutes. Afterwards, mice were injected with an average of 77.5 μCi of ^{18}F-NaF ion via tail vein injection using a tuberculin syringe, and maintained under anesthesia (2% isofluorane) on a heated induction chamber during the one-hour tracer uptake. All imaging chambers were calibrated and ARC-approved, and provided continuous delivery of anesthesia (2-2.5% isofluorane) with a controlled oxygen flow and temperature level of 36°C. All animals underwent micro-PET scanning (Siemens Medical Solutions Inc., TN, USA), followed by micro-computed tomography (micro-CT) scanning (Siemens Medical Solutions Inc., TN, USA) with a 10-min acquisition time for both scans. The animals were then placed in a recovery chamber and monitored closely for breathing. Micro-PET scan images were reconstructed using a filtered backprojection and iterative three-dimensional reconstruction technique (MAP) [52]. All animals were imaged at 2-week intervals starting at the baseline until the end of the study.

2.4.1 Quantitative analysis

Filtered backprojection images were used for quantification of tracer uptake. Plain anteroposterior radiographs (micro-CT) were superimposed on reconstructed PET images using A Medical Image Data Examiner (AMIDE) software version 0.7.15. Standardized region of interests (ROIs) were drawn in a box (4x6x4 mm^3) on a 3D view to encompass the distal femur-proximal tibia, and in another box (4x11x5 mm^3) to encompass lower lumbar vertebrae. Mean signal intensity (%ID/cc) within the volume of interest (VOI) was calculated using the AMIDE data analysis tool. Values were then corrected for the actual tracer injected dose. Rendered 3D images were generated by AMIDE, and a %ID/cc threshold of 80/3 was used.

2.5 Ex vivo assessment of bone architecture by micro computed tomography (micro-CT)

2.5.1 Specimen preparation for scanning

At the final time point, all mice were euthanized in a CO_2 chamber with the appropriate CO_2 concentrations and exposure times. Concomitantly, all organs were harvested and cleaned of soft tissue, then stored in 4% paraformaldehyde (PFA) at -4°C. After 48h, solutions were changed to 70% ethanol and stored at room temperature. In this study, a total of 26 femurs (both hindlimbs) and 13 vertebrae were scanned with Skyscan 1172 (Bruker microCT N.V., Belgium), equipped with a 5-μm focal spot microfocus x-ray tube at the resolution of 16μm

(55 kVp, 181 mA, and 0.5-mm Al Filter). Specimens were aligned with the vertical axis of the scanner, and low-density foam (a non-attenuating material) was used to stabilize the specimens firmly into a 0.25-diameter-tube. Phantom calibration was performed to relate the micro-CT values to a mineral-equivalent value (g/cm^3) of calcium hydroxyapatite (HA).

2.5.2 Reconstruction

For image processing, scanned images were reconstructed with NRecon (Bruker microCT N.V., Belgium) for attenuation correction, ring artifact reduction, and beam hardening. Following data acquisition, images were aligned in 3D view for vertical orientation with Data Viewer software for accuracy.

2.5.3 Segmentation of volume of interest

Image segmentation was performed manually by comparing the binarized image with the unsegmented image, and a single global threshold of 60 was applied. An irregular ROI selection was manually drawn parallel and close to the endocortical surface.

2.5.4 Ex vivo assessment of bone architecture by micro-CT analysis

Due to the differences in bone geometries in growing mice, length of the ROI was adjusted in proportion to the total femoral length and vertebral height. For distal femoral analyses, total length was approximately 2.5 mm with an offset of 1.5 mm to the growth plate. For L5, transverse micro-CT slices were acquired for the entire vertebral body, and trabecular bone was evaluated within the region of 0.3 mm away from the growth plate. To ensure accuracy, each ROI was drawn manually in a sequential manner for each transaxial micro-CT slice. Morphometric parameters were computed from the binarized images using a direct three-dimensional approach that does not rely on any prior assumptions about the underlying structure. For trabecular morphology, assessment of bone volume fraction (BV/TV, %), trabecular thickness (Tb. Th, mm), trabecular number (Tb. N, mm^{-1}), and trabecular separation (Tb. Sp, mm) were used. All analyses were performed with CTAn software (Bruker microCT N.V., Belgium).

2.5.5 Rendered 3D model construction

A 3D rendered model of femur and lumbar vertebrae was constructed by CTVol software (Bruker microCT N.V., Belgium). One representative sample was taken from each group. Comparison of the 3D rendered volume was performed to show differences in trabecular structure of the NELL-PEG-treated group and the PBS control.

2.6 Histology and quantitative histomorphometry

All right femurs were put in a 19% EDTA solution for 14 days and the solution was changed daily. Subsequently, all samples were sent to the Translational Pathology Core Laboratory (TPCL) at the UCLA Department of Pathology for paraffin embedding. Longitudinal sections of 5μm thickness were created by microtome. All slides were used for hematoxylin and eosin (H&E), trichrome, tartrate-resistant acid phosphatase (TRAP) and osteocalcin (OCN) staining. All specimens were analyzed under an Olympus BX51 microscope (Olympus Corp., Japan) using CellSens software version 1.6 (Olympus Corp., Japan). Six consecutive images at the distal femur region were acquired for OCN and TRAP analyses, which were completed by three blinded examiners using ImageJ software v1.48 (National Institute of Health, USA). Parameters of osteoblast number per trabecular bone surface (Ob. N/BS, mm^{-1}), osteoblast surface per trabecular bone surface (Ob. S/BS, mm), osteoclast number per trabecular bone surface (Oc. N/BS, mm^{-1}), and osteoclast surface per trabecular bone surface (Oc. S/BS, mm) were used.

2.7 Statistical analysis

Standard descriptive statistics and 95% confidence intervals were estimated, and the distributions of the parameters were assessed for normal distribution. For longitudinal data, percent change in each parameter over time was estimated using a linear mixed model. Independent sample t-tests were used to compare

means between the NELL-PEG-treated group and the PBS control group. Data are presented as mean± SEM, with * indicating $p<0.05$ and ** indicating $p<0.01$.

RESULTS

3.1 Biodistribution Study

Fig. 1 Biodistribution Study

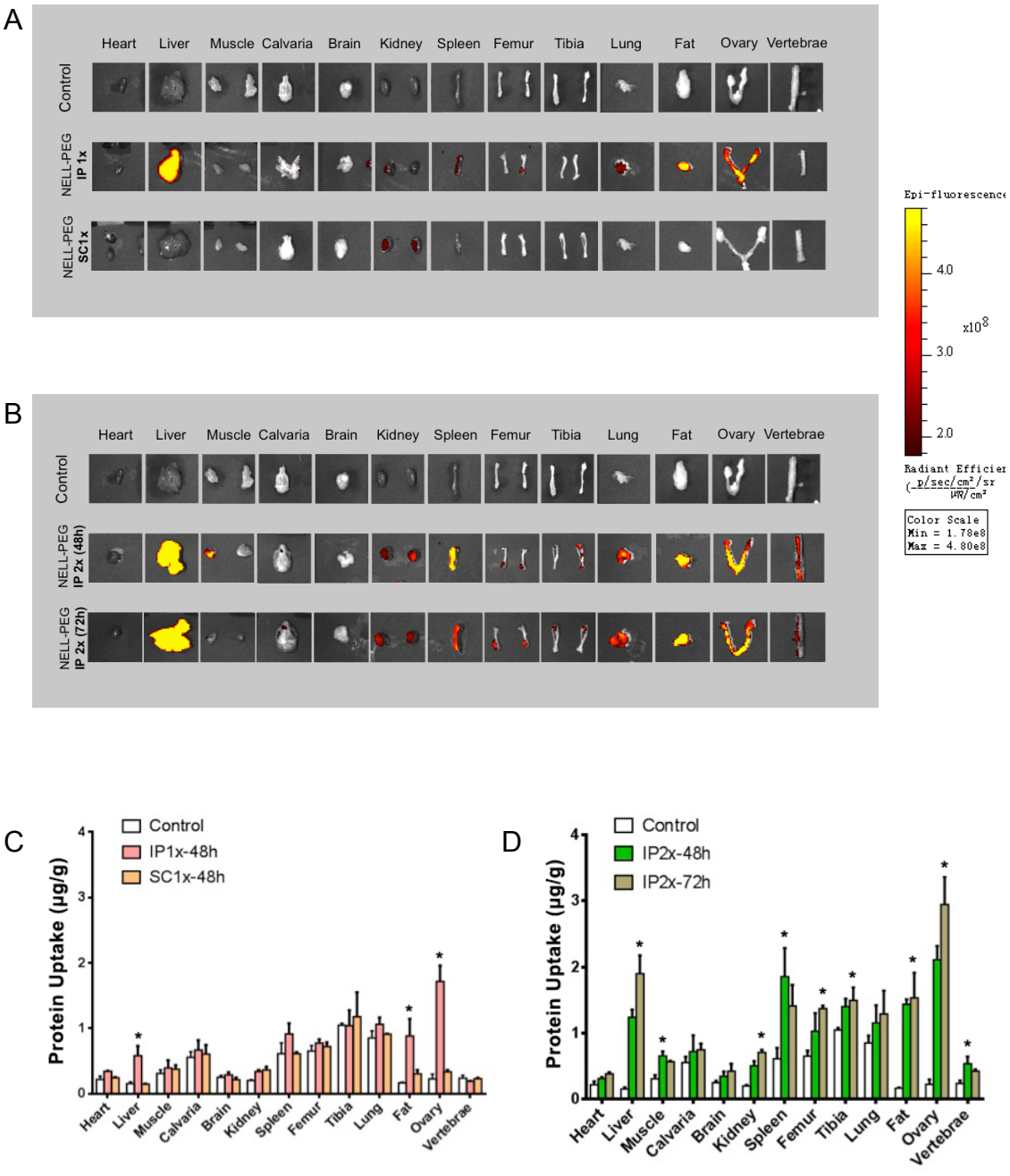

Fig. 1 Biodistribution study was performed to compare the protein distribution of NELL-PEG labeled with VivoTag680XL via the IP and SC administrations. (A) The IP and SC routes were compared after CD-1 mice were subjected to a single dose 1x (1.25 mg/kg) of NELL-PEG. *Ex vivo* images of the organs were collected at 48h post-injection. The IP injection group showed detectable protein retention on the organs of liver, spleen, kidney, lung, fat, ovary, and femur; however, a similar finding was not observed in the SC injection group. (B) A double dose 2x (2.5 mg/kg) of NELL-PEG was administered via the IP route, and the organs were dissected and imaged at two different time-points (48h and 72h) post-injection. (C) Quantification of the amount of protein distributed into different organs (μg/g). The biodistribution study confirmed that a single-dose injection of NELL-PEG via IP administration has significantly higher protein uptake in the liver, fat, and ovary when compared with the PBS control group. (D) A double dose injection of NELL-PEG via the IP administration showed that the quantification of the images at 48h post-injection has significantly higher protein uptake in the targeted bone tissues, namely femur, tibia, and vertebrae when compared with the control group. Quantification of the protein uptake at 72h post-injection revealed a higher amount of protein on the liver and kidney compared with the 48h post-injection. * Indicates significant difference ($p<0.05$) between treatment and control group means. Error bars represent standard deviation.

The biodistribution study was performed to compare the distribution of protein across various administration routes of NELL-PEG labeled with VivoTag680XL. The first part of the study compared a single dose (1.25 mg/kg) of NELL-PEG injection via the IP and SC injection routes (**Fig. 1A&1C**). *Ex vivo* fluorescence images at 48h post-injection showed a high hepatic uptake of the protein for a single-dose IP injection of NELL-PEG, suggesting that the protein was absorbed and highly metabolized by the liver. Other organs and tissues such as the spleen,

kidney, lung, fat, ovary, and femur also exhibited some protein retention (**Fig. 1A**). The fat and ovary also revealed high uptake due to their location near the injection site (**Fig. 1A**). The protein was not distributed to the liver via the SC injection route and there was no significant difference compared with the PBS control group, suggesting that the protein might have been degraded before it was absorbed into the capillaries (**Fig. 1A&1C**). Thus, the IP injection route was selected to further test the *in vivo* osteogenic potential of NELL-PEG with a double dose injection (2.5 mg/kg). To further examine the protein distribution of a double dose NELL-PEG injection via the IP route, the organs were harvested and imaged at two time-points, 48h and 72h (**Fig. 1B&1D**). At 48h post-injection, targeted bone tissues such as the femurs, tibias, and vertebrae exhibited a great amount of retention. On the other hand, images at 72h exhibited a greater amount of NELL-PEG in the liver and kidney compared with the images at 48h, suggesting not only a greater amount of protein was metabolized over a longer period of time, but also more protein was distributed to the overall organs (**Fig. 1D**).

3.2 Bone mineral density by DXA

Fig. 2 Bone mineral density by DXA

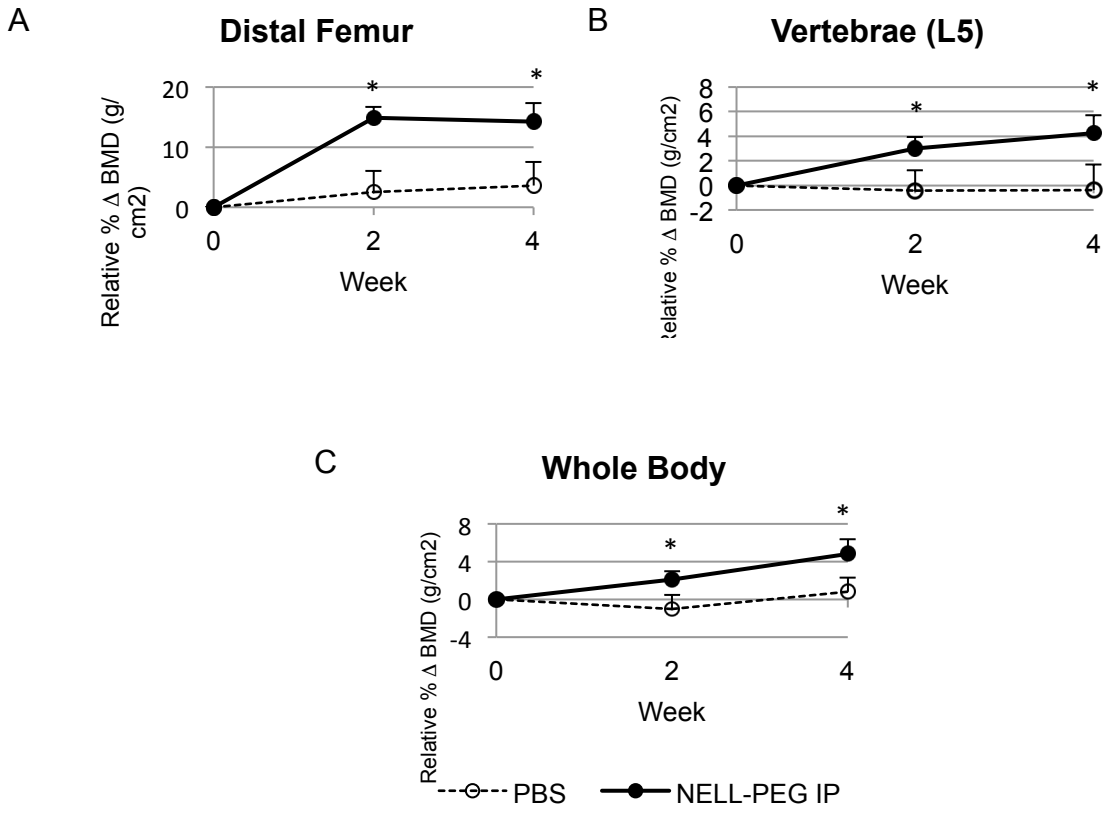

Fig. 2 To monitor the changes of BMD, DXA scan was performed. Presented are mean changes in trabecular bone mineral density at the second and fourth week of treatment for NELL-PEG-treated group and PBS control group at distal femoral metaphysis (A), fifth lumbar vertebral body (B), and the whole body (C). NELL-PEG-treated group is represented by solid line, whereas PBS control group is shown as dashed line. Compared with the control, NELL-PEG group shows significantly greater BMD increments relative to the week 0 baseline and it gradually increases until the end of the treatment. * Indicates significant difference ($p<0.05$) between treatment and control group means. Error bars represent standard error of the mean.

To dynamically monitor bone mineral density (BMD), DXA scans were performed throughout the study (**Fig. 2**). Weekly administration of NELL-PEG via the IP route revealed a significant increase of BMD in the distal femur beginning from the second week of treatment. By the fourth week, the relative BMD increased by 14.27% compared to week 0 baseline and then plateaued at a level significantly higher than that of the PBS control group (**Fig. 2A**). The increase in vertebral BMD followed a different pattern than that of the femoral BMD, sustaining a gradual increase up to 4.25% until the end of the treatment (**Fig. 2B**). Compared to the control, total BMD increased rapidly at each time point during treatment; meanwhile, the total BMD of the control group remained the same (**Fig. 2C**).

3.3 Bone turnover rate by live micro-PET/CT scanning with ^{18}F-NaF ion

Fig. 3 Bone turnover rate by live micro-PET/CT scanning with ^{18}F-NaF ion

A

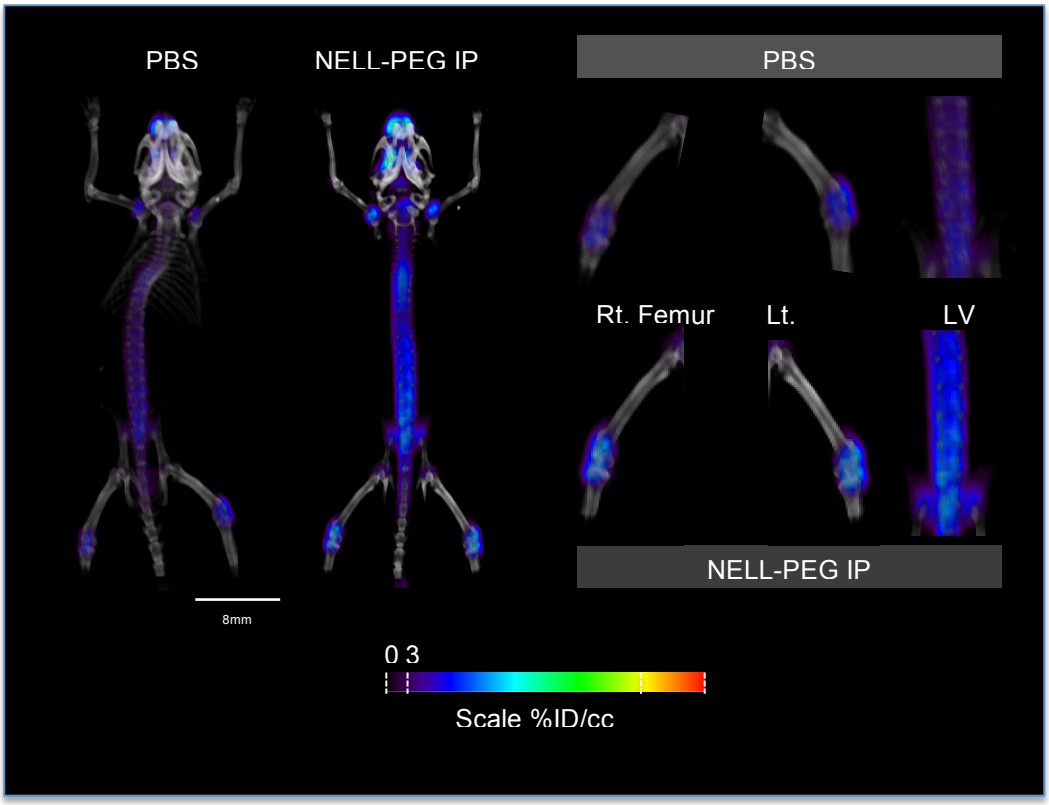

B

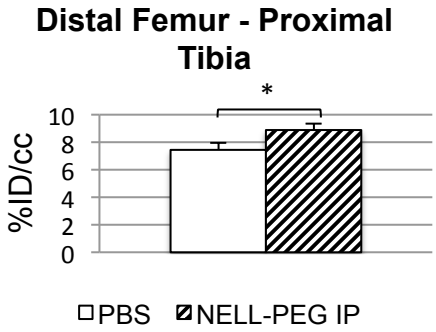

C

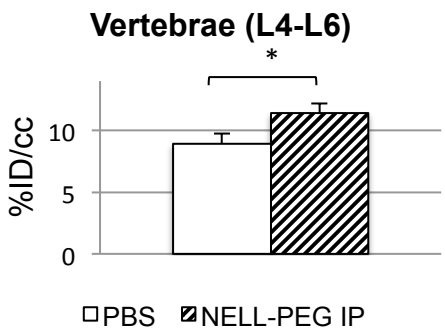

Fig. 3 (A) Representative live micro-PET/CT images of NELL-PEG-treated group revealed a higher uptake of ^{18}F-NaF ion over time, which corresponds to increased bone turnover rate in the targeted bone tissues, particularly the proximal humeri, vertebral body, distal femur, and proximal tibia when compared with the PBS control group. ROIs were drawn at the distal femur-proximal tibia region and the lower lumbar region to encompass the areas that show high signal intensity. (B&C) Quantification of mean value at the distal femur-proximal tibia region and lower lumbar region (%ID/cc) at the fourth week post-injection. NELL-PEG-treated group exhibited significantly greater concentration of ^{18}F-NaF ion uptake compared with the PBS control group. * Indicates significant difference ($p<0.05$) when compared with the control group. Error bars represent standard error of the mean.

Tracer uptake of ^{18}F-NaF was measured from the micro-PET/CT scans to assess the bone turnover rate. The results demonstrated that weekly injection of NELL-PEG increased the net uptake of ^{18}F-NaF ions at the final time point (**Fig. 3**). Overall, the micro-PET scans revealed increased signal intensity in the calvaria, the axial skeleton (thoracic and lumbar vertebrae), and around the growth plates of the appendicular bones such as the proximal humeri, distal femurs, and proximal tibia (**Fig. 3A**). Quantification of the mean value ratio at the distal femur-proximal tibia region of the treatment group exhibited significantly higher uptake of ^{18}F-NaF tracer in comparison to the control group (**Fig. 3B**). The lower lumbar vertebrae also revealed high signal intensity, with statistically significant differences between the two groups (**Fig. 3C**).

3.4 Bone architecture by micro-CT

Fig. 4 Bone architecture by micro-CT

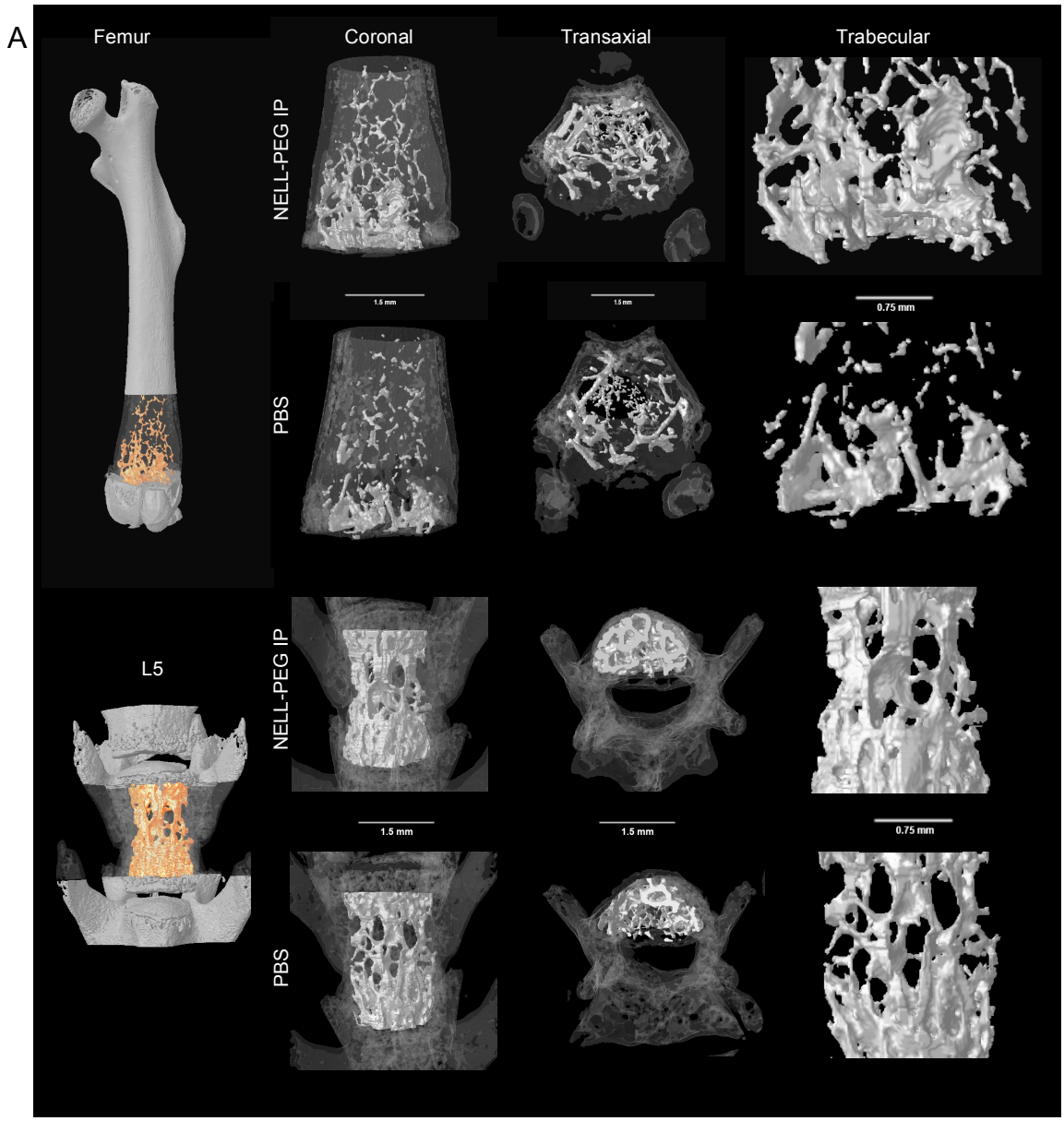

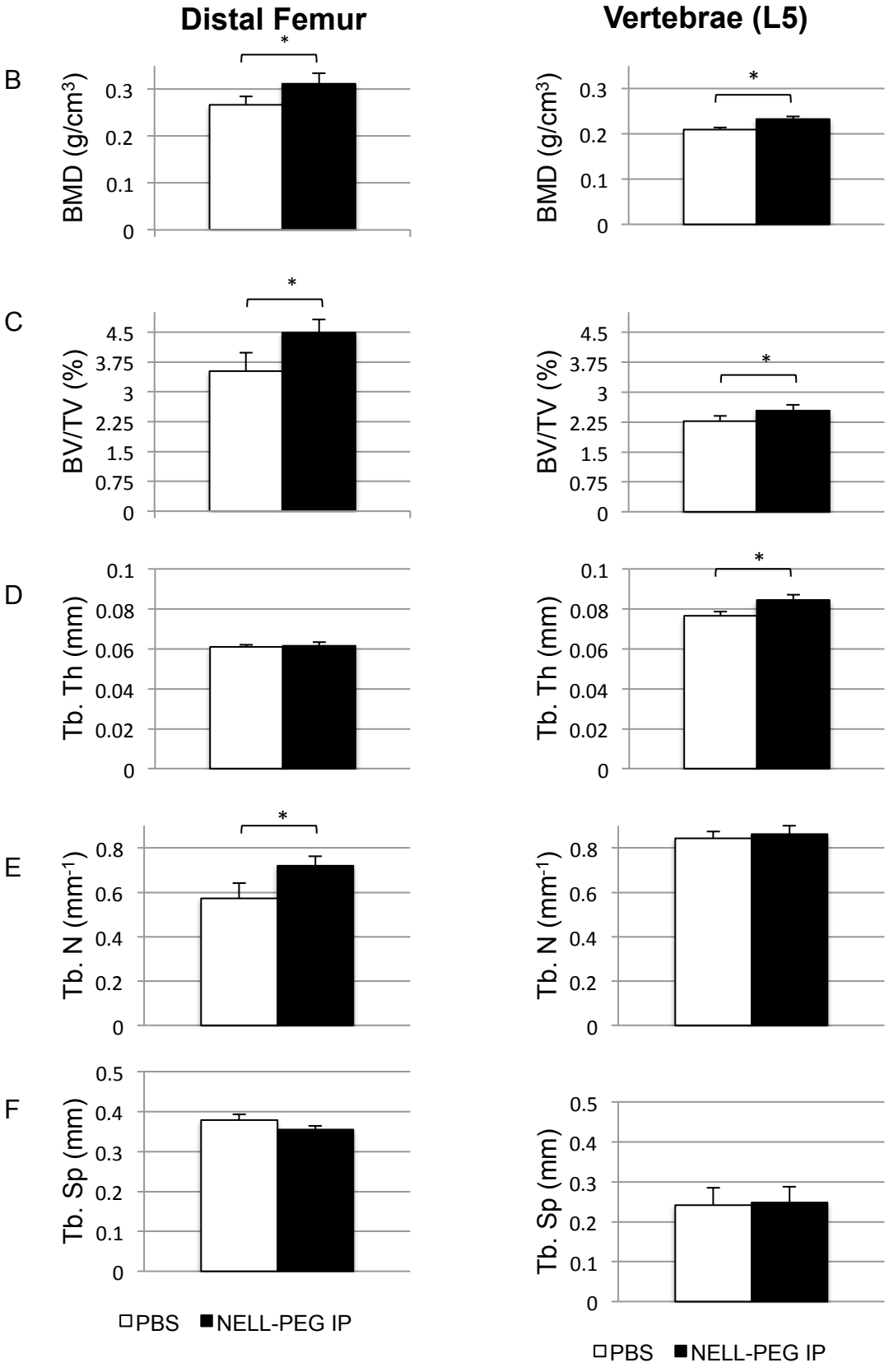
Distal Femur
Vertebrae (L5)
B
C
D
E
F
BMD (g/cm3)
BV/TV (%)
Tb. Th (mm)
Tb. N (mm-1)
Tb. Sp (mm)
*
PBS
NELL-PEG IP

Fig. 4 Ex vivo micro-CT results at the fourth week post-treatment. (A) Representative 3D volume rendered micro-CT images showing comparison of trabecular bone architecture at the distal femoral metaphysis and the lumbar vertebrae column (L5) in coronal and transaxial views. (A, rightmost column) Trabecular structure was magnified from each representative sample. (B-K) Trabecular bone architecture assessment by micro-CT for BMD, BV/TV, Tb. Th, Tb. N, and Tb. Sp. NELL-PEG group shows significant increases of BMD, BV/TV and improvement in trabecular structures at the distal femoral metaphysis and fifth vertebral column (L5) when compared with the PBS control group. * Indicates significant difference ($p<0.05$) when compared with the control group. Error bars represent standard error of the mean.

Comparisons of trabecular bone architecture at the distal femoral metaphysis region and the fifth lumbar region between the NELL-PEG injection group and the PBS control group are shown in **Fig. 4**. In the NELL-PEG group, robust trabecular bone formation was observed at the distal femoral metaphysis region (**Fig. 4A**). BMD was significantly greater in the NELL-PEG group (**Fig. 4B&4G**), which was consistent with our hindlimb and vertebrae DXA analyses. The trabecular morphology assessment demonstrated a statistically significant difference in bone volume fraction between the NELL-PEG group and the PBS control, indicating that there was a great amount of bone augmentation within the bone volume at the femurs and the vertebral body (**Fig. 4C&4H**). The trabecular bone architecture at the fifth lumbar vertebrae exhibited a significantly higher trabecular thickness when compared with the control (**Fig. 4I**). Similarly, the trabecular architecture at the distal femurs also exhibited a statistically significant difference when

compared with the control group (**Fig. 4E**). Overall, weekly NELL-PEG injection via the IP route significantly improved a number of bone architectural properties at the distal femur and lumbar vertebrae, confirmed by significant increases in BMD, bone volume fraction, and trabecular bone parameters at the end of the treatment.

3.5 Bone remodeling activity by histology and immunohistochemistry

Fig. 5 Bone remodeling activity by histology and immunohistochemistry

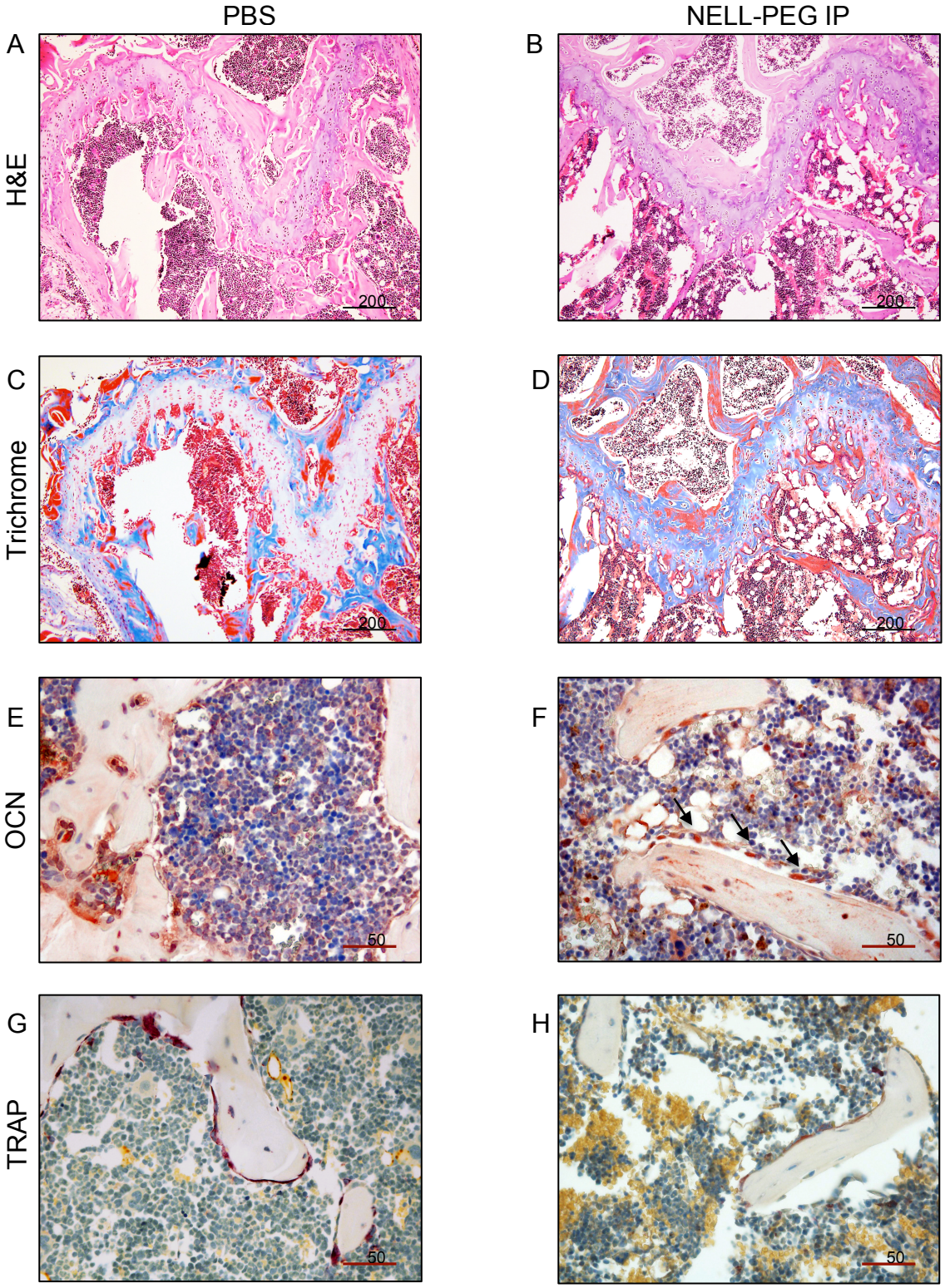

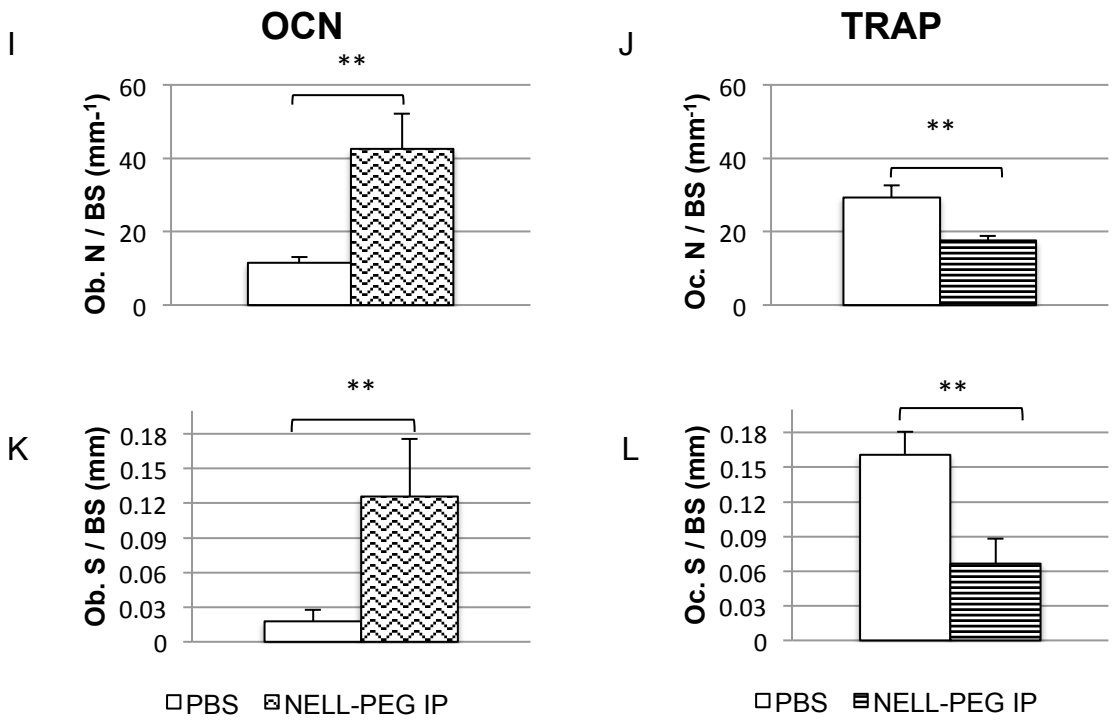

Fig. 5 Histological analyses of distal femoral metaphysis in NELL-PEG treated group and control. (A&B) H&E staining (bar, 200 μm) and (C&D) Trichrome staining (bar, 200 μm) at the growth plate region shows more trabecular bone formation in the NELL-PEG group when compared with the PBS control. (E&F) High power view of OCN staining (bar, 50 μm) shows more osteoblasts in treated group (shown with arrows). (G&H) TRAP staining (bar, 50 μm) reveals more osteoclasts in the control group as compared with the NELL-PEG injection group. (I-L) Quantification of bone remodeling process parameters that include osteoblast number per trabecular bone surface (Ob. N/BS, mm^{-1}), osteoblast surface per trabecular bone surface (Ob. S/BS, mm), osteoclast number per trabecular bone surface (Oc. N/BS, mm^{-1}), and osteoclast surface per trabecular bone surface (Oc. S/BS, mm). ** Indicates significant difference ($p<0.01$) when compared with the control group. Error bars represent standard error of the mean.

To assess the underlying cellular mechanisms of the bone remodeling process, histological analysis and static indices assessment at the distal femoral metaphysis region were performed (**Fig. 5)**. Consistent with the micro-CT findings, histological analysis exhibited a significant increase of trabecular bone formation in the NELL-PEG-treated group when compared with the PBS control (**Fig. 5A**&**5B**). Low magnification view of the distal femoral metaphysis region stained with trichrome revealed actively remodeling bone in the NELL-PEG treated group (**Fig. 5C**&**5D**). Accordingly, results from OCN staining exhibited greater active bone formation (**Fig. 5E&5F**), aligning with the results from TRAP staining that exhibited less osteoclastic activity in the treated group relative to the control (**Fig. 5G&5H**). The bone remodeling process parameters that include osteoblast number per trabecular bone surface (Ob.N/BS, mm^{-1}), osteoblast surface per trabecular bone surface (Ob.S/BS, mm), osteoclast number per trabecular bone surface (Oc.N/BS, mm^{-1}), and osteoclast surface per trabecular bone surface (Oc.S/BS, mm) all demonstrated that the NELL-PEG treated group had a higher number of bone remodeling process indices when compared with the control.

DISCUSSION

Consistent with our previous findings, the results from this study demonstrate the ability of NELL-PEG to enhance bone quantity and quality by increasing osteoblast activity and suppressing osteoclast activity. These findings demonstrate that NELL-PEG has the potential to be a novel osteoporosis therapy with both anabolic and antiresorptive functions, in accordance with literatures [2, 10, 12-14, 38-42]. While once-every-2-day (q2d) IV tail administration of unmodified NELL-1 has proven to be successful, the half-life of naked NELL-1 was relatively short (5.5 hours), thereby limiting its clinical use and therapeutic applications due to the burden of frequent administration [10]. In order to improve the pharmacokinetics of NELL-1 by prolonging its half-life without diminishing its osteogenic potential, we utilized the FDA-approved method of PEGylation to conjugate NELL-1 with PEG, a water-soluble polymer [11, 12]. The half-life of NELL-PEG 5K (linear PEG-NHS with *Mw* 5kDa) was increased to 14.5 hours, allowing the protein to be administered weekly as opposed to every other day [11, 12]. The present study revealed that a weekly injection of double dose NELL-PEG via the IP injection route successfully increases BMD and trabecular bone formation with reduced bone resorption, suggesting that IP administration of NELL-PEG serves as an effective approach that can be further developed into a systemic therapy for osteoporosis.

Many studies have shown the efficacy of various drug administration routes for drug delivery in mice. However, thus far there are only a few studies that compare the effects of different administration routes on bone tissue regeneration. Here, we attempted to overcome this issue by comparing the IP and SC administration of NELL-PEG and by examining the effects of a weekly double dose NELL-PEG IP administration on the overall bone quality after four weeks of treatment. In laboratory setting, IV, IP and SC routes constitute the most frequently used drug delivery methods [49]. IV administration is commonly used because it circumvents first-pass metabolism by the liver, thereby allowing for rapid dispersal of the drug into the entire circulatory system subsequently after injection. However, in addition to difficult manipulation, there are noteworthy risks of inflammation, thrombophlebitis of the vein, and necrosis of the surrounding tissues. On the other hand, IP administration is less invasive than IV administration and facilitates absorption due to the large surface area of the abdominal cavity and abundant blood supply at the injection site. It is important to note that the drug absorption rate depends on factors such as the route of administration and the dosage. For IP administration, the absorption rate is one-half to one-fourth compared to that of IV administration [49]. Conversely, SC administration has the slowest rate of absorption when compared to the IV and IP routes. Compared with the IV route, the IP and SC routes are more favorable for drug delivery because they are not only less invasive, but also allow for a greater volume of injection that serves as a slow-release and long-acting deposit of the drug [49, 50]. For long-term drug delivery formulations in humans, factors such as the safety profile of the drug,

ease of administration, subject accessibility and mobility, target area and injection site, and cost of the therapy should be taken into consideration. Nonetheless, in laboratory settings, the IP route has been more widely used for drug delivery due to its induction of greater effects in a shorter period of time [48-51].

In the biodistribution study, imaging of the organs *ex vivo* was conducted at 48h post-injection of the single dose of NELL-PEG (1.25 mg/kg) via IP and SC administration (**Fig. 1A**). In comparison to the SC administration group, the IP group showed a greater NELL-PEG signal intensities in the liver, fat, and ovary when compared to the control, suggesting that the protein was absorbed and metabolized via the IP route, but not via the SC route (**Fig. 1C**). In general, the liver and spleen were able to uptake large quantities of protein at 48h post-injection for the IV and IP administrations, but this was not observed in the SC administration. This observation may be attributable to the high molecular weight of NELL-PEG (863.1 kDa), which hinders diffusion into the capillaries near the injection site and subsequent distribution by the systemic circulation. To observe the efficacy and distribution of NELL-PEG uptake via the IP route, the dose was doubled (2.5 mg/kg) and imaging was conducted at two different time points (48h and 72h) post-injection. Upon IP injection of the double dose (2.5 mg/kg), bioluminescence imaging at 48h post-injection revealed a high concentration of NELL-PEG in the targeted bone tissues such as the calvaria, vertebrae, femur, and tibia (**Fig. 1B**). To further investigate the protein retention period and its distribution into the targeted tissues, the organs were also imaged

at 72h post-injection. At this time, there was a higher signal intensity for the overall organs, particularly the calvaria, vertebrae, and femur when compared to the images at 48h post-injection (**Fig. 1D**). These findings suggest injection of NELL-PEG via the IP route can facilitate the slow absorption of the protein from the injection site, thus maintaining a high-level protein concentration for a longer period of time. Taken together with our previous data, these novel findings led us to further examine the applicability of NELL-PEG injection via the IP route using an *in vivo* mouse model.

Our *in vivo* data demonstrate that a weekly IP double-dose (2.5 mg/kg) administration of NELL-PEG successfully increases BMD in the targeted bone sites, particularly the distal femur and the fifth lumbar vertebrae. This observation is consistent with our previous findings on NELL-PEG injection via the IV route [12]. Overall, the total BMD increased significantly beginning from the second week of treatment when compared to the PBS control group, and was sustained until the end of the treatment (**Fig. 2**). To evaluate the profound effect of NELL-PEG on bone remodeling and its effects on bone quality, it is essential to investigate the bone turnover rate. Thus, we performed micro-PET/CT scans with a radiolabeled tracer of ^{18}F-NaF, a positron-emitting radiopharmaceutical tracer that is carried through the blood stream upon systemic administration and binds to the bone surface through the ion exchange of hydroxyl (OH^-) exchange with hydroxyapatite. As a result, it forms a fluoroapatite that integrates with bone matrix formation [53]. Tracer uptake of ^{18}F-NaF corresponds to the bone turnover

process that involves osteoblastic and osteoclastic activities on the bone surface, which concomitantly reflects the bone remodeling process [53-56]. In the present study, a double dose injection of NELL-PEG via the IP route revealed a higher intensity of tracer uptake throughout the overall body when compared to the PBS control group (**Fig. 3**). This finding suggests that the NELL-PEG-treated animals exhibited greater bone remodeling process than the animals in the control group.

Furthermore, microCT data showed that weekly NELL-PEG administration via the IP route promotes dramatic improvement in bone quality at the long bone sites by significantly escalating BMD and inducing robust trabecular bone formation (**Fig. 4**). In particular, the trabecular structures at the distal femur and the fifth lumbar vertebrae showed comparatively linear results. In general, IP injection of NELL-PEG was found to improve bone quality at multiple skeletal sites, suggesting the potential of NELL-PEG to serve as an effective osteoporosis therapy. These microCT results were similar to the results found of the single-dose NELL-PEG IV injection from our recently published data [12]. Specifically, the percent increase of BMD at the distal femurs of the double dose IP injection was comparable to that of the single dose of IV injection. To evaluate the anabolic and anti-resorptive effects of NELL-PEG injection on the bone remodeling process, histological analyses were performed at the distal femoral metaphysis region. The results from the histological analyses were consistent with the aforementioned findings that there was a significant increase in bone formation due to an increase in osteoblastic activity and reduced

osteoclast-induced bone resorption (**Fig. 5**). As a whole, these findings indicate that an active bone remodeling process occurred at the targeted bone sites after NELL-PEG IP administration.

CONCLUSION

In summary, our results indicate that NELL-PEG injection via IP administration results in a greater uptake when compared with NELL-PEG injection via SC administration, and higher protein retention at multiple skeletal sites such as the calvaria, vertebral body, and femur. In addition, we have demonstrated that weekly IP administration of double dose NELL-PEG successfully enhances bone mineral density, relative volume of calcified tissue, and osteoblast activities, while reducing osteoclast activities in the targeted bone sites. This is comparable to a single dose NELL-PEG treatment via IV administration as previously demonstrated by our group. Altogether, these findings suggest that IP administration is an excellent alternative method to systemically deliver NELL-PEG for osteoporosis therapy.

REFERENCES

[1] Ting K, Vastardis H, Mulliken JB, Soo C, Tieu A, Do H, et al. Human NELL-1 expressed in unilateral coronal synostosis. Journal of bone and mineral research : the official journal of the American Society for Bone and Mineral Research. 1999;14:80-9.

[2] Zhang X, Zara J, Siu RK, Ting K, Soo C. The role of NELL-1, a growth factor associated with craniosynostosis, in promoting bone regeneration. Journal of dental research. 2010;89:865-78.

[3] Aghaloo T, Cowan CM, Chou YF, Zhang X, Lee H, Miao S, et al. Nell-1-induced bone regeneration in calvarial defects. Am J Pathol. 2006;169:903-15.

[4] Cowan CM, Zhang X, James AW, Kim TM, Sun N, Wu B, et al. NELL-1 increases pre-osteoblast mineralization using both phosphate transporter Pit1 and Pit2. Biochemical and biophysical research communications. 2012;422:351-7.

[5] Kwak J, Zara JN, Chiang M, Ngo R, Shen J, James AW, et al. NELL-1 injection maintains long-bone quantity and quality in an ovariectomy-induced osteoporotic senile rat model. Tissue engineering Part A. 2013;19:426-36.

[6] Li W, Lee M, Whang J, Siu RK, Zhang X, Liu C, et al. Delivery of lyophilized Nell-1 in a rat spinal fusion model. Tissue engineering Part A. 2010;16:2861-70.

[7] Lu SS, Zhang X, Soo C, Hsu T, Napoli A, Aghaloo T, et al. The osteoinductive properties of Nell-1 in a rat spinal fusion model. The spine journal : official journal of the North American Spine Society. 2007;7:50-60.

[8] Siu RK, Lu SS, Li W, Whang J, McNeill G, Zhang X, et al. Nell-1 protein promotes bone formation in a sheep spinal fusion model. Tissue engineering Part A. 2011;17:1123-35.

[9] Aghaloo T, Jiang X, Soo C, Zhang Z, Zhang X, Hu J, et al. A study of the role of nell-1 gene modified goat bone marrow stromal cells in promoting new bone formation. Molecular therapy : the journal of the American Society of Gene Therapy. 2007;15:1872-80.

[10] James AW, Shen J, Zhang X, Asatrian G, Goyal R, Kwak JH, et al. NELL-1 in the treatment of

osteoporotic bone loss. Nature communications. 2015;6:7362.

[11] Zhang Y, Velasco O, Zhang X, Ting K, Soo C, Wu BM. Bioactivity and circulation time of PEGylated NELL-1 in mice and the potential for osteoporosis therapy. Biomaterials. 2014;35:6614-21.

[12] Kwak JH, Zhang Y, Park J, Chen E, Shen J, Chawan C, et al. Pharmacokinetics and osteogenic potential of PEGylated NELL-1 in vivo after systemic administration. Biomaterials. 2015;57:73-83.

[13] Zhang X, Ting K, Bessette CM, Culiat CT, Sung SJ, Lee H, et al. Nell-1, a key functional mediator of Runx2, partially rescues calvarial defects in Runx2(+/-) mice. Journal of bone and mineral research : the official journal of the American Society for Bone and Mineral Research. 2011;26:777-91.

[14] James AW, Pan A, Chiang M, Zara J, Zhang X, Ting K, et al. A new function of Nell-1 protein in repressing adipogenic differentiation. Biochemical and biophysical research communications. 2011.

[15] Karasik D, Hsu YH, Zhou Y, Cupples LA, Kiel DP, Demissie S. Genome-wide pleiotropy of osteoporosis-related phenotypes: the Framingham Study. Journal of bone and mineral research : the official journal of the American Society for Bone and Mineral Research. 2010;25:1555-63.

[16] Reginster JY, Burlet N. Osteoporosis: a still increasing prevalence. Bone. 2006;38:S4-9.

[17] Heinemann DF. Osteoporosis. An overview of the National Osteoporosis Foundation clinical practice guide. Geriatrics. 2000;55:31-6; quiz 9.

[18] Czerwinski E, Badurski JE, Marcinowska-Suchowierska E, Osieleniec J. Current understanding of osteoporosis according to the position of the World Health Organization (WHO) and International Osteoporosis Foundation. Ortopedia, traumatologia, rehabilitacja. 2007;9:337-56.

[19] Watts NB, Lewiecki EM, Miller PD, Baim S. National Osteoporosis Foundation 2008 Clinician's Guide to Prevention and Treatment of Osteoporosis and the World Health Organization Fracture Risk Assessment Tool (FRAX): what they mean to the bone densitometrist and bone technologist. Journal of clinical densitometry : the official journal of the International Society for Clinical Densitometry. 2008;11:473-7.

[20] Berry SD, Kiel DP, Donaldson MG, Cummings SR, Kanis JA, Johansson H, et al. Application of the National Osteoporosis Foundation Guidelines to postmenopausal women and men: the Framingham

Osteoporosis Study. Osteoporosis international : a journal established as result of cooperation between the European Foundation for Osteoporosis and the National Osteoporosis Foundation of the USA. 2010;21:53-60.

[21] Pearsall RS, Canalis E, Cornwall-Brady M, Underwood KW, Haigis B, Ucran J, et al. A soluble activin type IIA receptor induces bone formation and improves skeletal integrity. Proceedings of the National Academy of Sciences of the United States of America. 2008;105:7082-7.

[22] Jilka RL. Molecular and cellular mechanisms of the anabolic effect of intermittent PTH. Bone. 2007;40:1434-46.

[23] Neer RM, Arnaud CD, Zanchetta JR, Prince R, Gaich GA, Reginster JY, et al. Effect of parathyroid hormone (1-34) on fractures and bone mineral density in postmenopausal women with osteoporosis. The New England journal of medicine. 2001;344:1434-41.

[24] Bilezikian JP. Combination anabolic and antiresorptive therapy for osteoporosis: opening the anabolic window. Current osteoporosis reports. 2008;6:24-30.

[25] Cusano NE, Bilezikian JP. Combination anabolic and antiresorptive therapy for osteoporosis. Endocrinology and metabolism clinics of North America. 2012;41:643-54.

[26] Zhou H, Iida-Klein A, Lu SS, Ducayen-Knowles M, Levine LR, Dempster DW, et al. Anabolic action of parathyroid hormone on cortical and cancellous bone differs between axial and appendicular skeletal sites in mice. Bone. 2003;32:513-20.

[27] Cairoli E, Zhukouskaya VV, Eller-Vainicher C, Chiodini I. Perspectives on osteoporosis therapies. Journal of endocrinological investigation. 2015;38:303-11.

[28] Ishtiaq S, Fogelman I, Hampson G. Treatment of post-menopausal osteoporosis: beyond bisphosphonates. Journal of endocrinological investigation. 2015;38:13-29.

[29] Lippuner K. The future of osteoporosis treatment - a research update. Swiss medical weekly. 2012;142:w13624.

[30] Kennel KA, Drake MT. Adverse effects of bisphosphonates: implications for osteoporosis management. Mayo Clinic proceedings. 2009;84:632-7; quiz 8.

[31] Papapetrou PD. Bisphosphonate-associated adverse events. Hormones. 2009;8:96-110.

[32] Minear S, Leucht P, Jiang J, Liu B, Zeng A, Fuerer C, et al. Wnt proteins promote bone regeneration. Science translational medicine. 2010;2:29ra30.

[33] Wagner ER, Zhu G, Zhang BQ, Luo Q, Shi Q, Huang E, et al. The therapeutic potential of the Wnt signaling pathway in bone disorders. Current molecular pharmacology. 2011;4:14-25.

[34] Bone HG, McClung MR, Roux C, Recker RR, Eisman JA, Verbruggen N, et al. Odanacatib, a cathepsin-K inhibitor for osteoporosis: a two-year study in postmenopausal women with low bone density. Journal of bone and mineral research : the official journal of the American Society for Bone and Mineral Research. 2010;25:937-47.

[35] Feng S, Luo Z, Liu D. Efficacy and safety of odanacatib treatment for patients with osteoporosis: a meta-analysis. Journal of bone and mineral metabolism. 2015;33:448-54.

[36] Gajic-Veljanoski O, Tomlinson G, Srighanthan J, Adachi JD, Josse R, Brown JP, et al. Effect of odanacatib on BMD and fractures: estimates from Bayesian univariate and bivariate meta-analyses. The Journal of clinical endocrinology and metabolism. 2014;99:3070-9.

[37] Evenepoel P, D'Haese P, Brandenburg V. Romosozumab in postmenopausal women with osteopenia. The New England journal of medicine. 2014;370:1664.

[38] Shen J, James AW, Zara JN, Asatrian G, Khadarian K, Zhang JB, et al. BMP2-induced inflammation can be suppressed by the osteoinductive growth factor NELL-1. Tissue engineering Part A. 2013;19:2390-401.

[39] James AW, Pang S, Askarinam A, Corselli M, Zara JN, Goyal R, et al. Additive effects of sonic hedgehog and Nell-1 signaling in osteogenic versus adipogenic differentiation of human adipose-derived stromal cells. Stem cells and development. 2012;21:2170-8.

[40] Truong T, Zhang X, Pathmanathan D, Soo C, Ting K. Craniosynostosis-associated gene nell-1 is regulated by runx2. Journal of bone and mineral research : the official journal of the American Society for Bone and Mineral Research. 2007;22:7-18.

[41] Chen W, Zhang X, Siu RK, Chen F, Shen J, Zara JN, et al. Nfatc2 is a primary response gene of Nell-1 regulating chondrogenesis in ATDC5 cells. Journal of bone and mineral research : the official journal of the

American Society for Bone and Mineral Research. 2011;26:1230-41.

[42] Shen J, James AW, Chung J, Lee K, Zhang JB, Ho S, et al. NELL-1 promotes cell adhesion and differentiation via Integrinbeta1. Journal of cellular biochemistry. 2012;113:3620-8.

[43] James AW, Pan A, Chiang M, Zara JN, Zhang X, Ting K, et al. A new function of Nell-1 protein in repressing adipogenic differentiation. Biochemical and biophysical research communications. 2011;411:126-31.

[44] Harris JM, Chess RB. Effect of pegylation on pharmaceuticals. Nature reviews Drug discovery. 2003;2:214-21.

[45] Pasut G, Guiotto, A., Veronese, FM. Protein, peptide and non-peptide drug PEGylation for therapeutic application. Expert Opinion on Therapeutic Patents. 2004;14:859-94.

[46] Veronese FM, Mero A. The impact of PEGylation on biological therapies. BioDrugs : clinical immunotherapeutics, biopharmaceuticals and gene therapy. 2008;22:315-29.

[47] Zhao LS, Yin R, Wei BB, Li Q, Jiang ZY, Chen XH, et al. Comparative pharmacokinetics of cefuroxime lysine after single intravenous, intraperitoneal, and intramuscular administration to rats. Acta pharmacologica Sinica. 2012;33:1348-52.

[48] de Bekker-Grob EW, Essink-Bot ML, Meerding WJ, Pols HA, Koes BW, Steyerberg EW. Patients' preferences for osteoporosis drug treatment: a discrete choice experiment. Osteoporosis international : a journal established as result of cooperation between the European Foundation for Osteoporosis and the National Osteoporosis Foundation of the USA. 2008;19:1029-37.

[49] Woodard G. Principles in Drug Administration. Methods of Animal Experimentation1965. p. 343-59.

[50] Mitra A, Lee, CH., Cheng, K. Advanced Drug Delivery: Wiley; 2013.

[51] Shuid AN, Ibrahim N, Mohd Amin MC, Mohamed IN. Drug delivery systems for prevention and treatment of osteoporotic fracture. Current drug targets. 2013;14:1558-64.

[52] Chatziioannou A, Silverman, RW., Meadors, K., Farquhar, TH, Cherry, SR. Techniques to improve the spatial sampling of MicroPET-a high resolution animal PET tomograph. Nuclear Science. 2000;47:422-7.

[53] Hsu WK, Feeley BT, Krenek L, Stout DB, Chatziioannou AF, Lieberman JR. The use of 18F-fluoride and

18F-FDG PET scans to assess fracture healing in a rat femur model. European journal of nuclear medicine and molecular imaging. 2007;34:1291-301.

[54] Bastawrous S, Bhargava P, Behnia F, Djang DS, Haseley DR. Newer PET application with an old tracer: role of 18F-NaF skeletal PET/CT in oncologic practice. Radiographics : a review publication of the Radiological Society of North America, Inc. 2014;34:1295-316.

[55] Frost ML, Siddique M, Blake GM, Moore AE, Schleyer PJ, Dunn JT, et al. Differential effects of teriparatide on regional bone formation using (18)F-fluoride positron emission tomography. Journal of bone and mineral research : the official journal of the American Society for Bone and Mineral Research. 2011;26:1002-11.

[56] Czernin J, Satyamurthy N, Schiepers C. Molecular mechanisms of bone 18F-NaF deposition. Journal of nuclear medicine : official publication, Society of Nuclear Medicine. 2010;51:1826-9.